Meteoritics & Planetary Science 39, Nr 2, 267–286 (2004)
Abstract available online at http://meteoritics.org

Structural evidence from shock metamorphism in simple and complex impact craters: Linking observations to theory

Michael R. DENCE

824 Nesbitt Place, Ottawa, Ontario K2C 0K1, Canada
E-mail: mrdence@rsc.ca

(Received 28 July 2003; revision accepted 15 December 2003)

Abstract–The structure of Canadian impact craters formed in crystalline rocks is analyzed using shock metamorphism and evidence for movement along shear zones. The analysis is based on an interpretation that, beyond the near field region, shock pressure attenuates down axis as $P \sim R^{-2}$, in agreement with nuclear test and computed results, and as $P \sim R^{-3}$ near the surface. In both simple and complex craters, the transient cavity is defined by the limit of fragmentation due to direct and reflected shock waves. The intersection of the transient cavity with hemispheric shock isobars indicates that the transient cavity has a parabolic form. Weakening by dilation during early uplift allows late stage slumping of the walls of simple craters. This is controlled by a spheroidal primary shear of radius $r_s \approx 2d_t$, where d_t is the depth of the transient crater due to excavation and initial compression. With increasing crater diameter, the size of the transient cavity decreases relative to the shock imprint, suggesting that fragmentation and excavation is limited by progressively earlier collapse of the margins under gravity. Central peak formation in complex craters may be initiated by relaxation of the shock-compressed central parautochthone, so the primary shear, lubricated by friction melting, meets below the crater floor and drives the continuing upward motion.

PREFACE

The admirable objective of bringing together theoreticians, modelers, and observers to ponder the state of understanding of hypervelocity impact craters follows an equally admirable tradition exemplified by the meetings convened by French and Short (1968) and Roddy et al. (1977). New perspectives have been the lifeblood of impact crater research, a field that has had more than its share of battles generated by old prejudices and remarkable blind spots. Bob Dietz brought a fresh viewpoint to Sudbury and was rewarded by the discovery of shatter cones (Dietz 1964) that legions of geologists had passed over in 80 years of detailed mapping. At about the same time, Jehan Rondot was in the midst of routine regional mapping in the Charlevoix region. He recognized unusual fracture patterns in a well-exposed roadside outcrop and later learned from John Murtaugh (who was mapping Manicouagan at the time) that he had discovered shatter cones (Rondot 1966). Thereby, Rondot added to the growing Canadian list a large impact site that was previously unrecognized despite 15 years of systematic searching for likely structures on the Canadian shield (Beals 1965).

Charlevoix resembles Sudbury in that both have been affected by subsequent tectonic events that add to the challenge of interpretation. They remind us that each impact site has unique features and settings that pose problems for those seeking a general theory. The selection made here is an attempt to identify data for which such problems seem relatively manageable and so bear directly on the task of bridging the gap to theory. A robust understanding of the craters within the range surveyed in this paper is essential for probing the mysteries of the largest structures, such as Chicxulub, Vredefort, and Sudbury. It is my prejudice that Sudbury, in particular, has further surprises in store and is far from a straightforward extrapolation from craters half its size. An ultimate aim, therefore, is to test this view and decide if the recipe for Sudbury requires more of the same or additional ingredients.

INTRODUCTION

This review surveys aspects of the Canadian experience in studying craters formed in Precambrian crystalline rocks of the Canadian Shield (Beals et al. 1963). It outlines some of the successes and difficulties experienced by earlier analyses of impact crater mechanics as the database grew (Dence 1968; Dence et al. 1977; Grieve et al. 1981) and expands on

© Meteoritical Society, 2004. Printed in USA.

recent revisions and additions to these analyses (Dence 2002). In particular, it summarizes the use of shock metamorphism data in illuminating impact crater structure and mechanics and highlights assumptions made in translating surface and drill core observations into relevant structural data.

An initial assumption is that, for the most part, the crystalline rocks of the Shield can be treated as physically homogeneous and isotropic. Such a view is encouraged by the general similarity of features observed in craters of comparable size, after due allowance for erosion and state of preservation, in Canada and elsewhere in similar settings (e.g., Boltysh; Grieve et al. 1987; Kelley and Gurov 2002). It follows that, for these target materials, changes in form and structure with size can be analyzed largely as functions of energy rather than possible differences in target material properties. This is generally not the case where sedimentary rocks with varying physical properties are a substantial proportion of the country rocks, as at Canadian craters such as Carswell (Innes 1964) and Haughton (Robertson 1988). For the largest terrestrial craters, notably Sudbury, additional factors such as the regional thermal gradient at the time of impact and bulk changes in composition of the lithosphere have to be taken into account. These situations are not considered in the present analysis.

In general, the rocks of the Canadian Shield lack structures that can provide direct information about pre-impact configuration. The exceptions are a few cases where, at the time of impact, the Precambrian basement was overlain by relatively thin (100–200 m thick) sequences of flat-lying Paleozoic sedimentary rocks. These provide important indicators of the final disposition and conformation of the original surface, but, as they are a minor component of the target, they appear to have little influence on the final crater form.

The impact craters that form the core of the database from the Canadian Shield are listed in Table 1, while some comparable craters from other parts of the world are noted in Table 2. Note that some diameters and ages differ from those given in the standard Earth Impact Database. A brief reason for the preferences used here is given in the attached notes. Though the extent of erosion differs, the Canadian craters are sufficiently well preserved to demonstrate the topographic range identified on other planets, from simple to central peak and peak ring forms, as a function of increasing size. The present inquiry concentrates on internal changes in structure that likewise change with size and thereby shed light on crater mechanics. Ejecta are not considered, as glacial erosion has stripped any such deposits from the exterior of all the Canadian craters. Glacial action has similarly eroded most interior impact breccia deposits except where protected by post-impact sedimentary fill.

Terminology

In this review, a distinction is maintained between fragmentation, leading to the formation of allogenic breccias and fracturing associated with faults, shears, and some localized autochthonous, usually monomict breccias. Layers of impact-produced melt rocks and associated breccias within craters are collectively referred to as allochthonous deposits. Where the uppermost layers are preserved, they may include

Table 1. Representative Canadian impact craters.[a]

Name	Morphological type	Location	Diameter (km)	Age (Myr)
Holleford, Ontario	Simple	N 44°28′ W 76°38′	2.35	550 ± 100
West Hawk Lake, Manitoba	Simple	N 49°46′ W 95°11′	2.44	100 ± 50
New Quebec, Quebec	Simple	N 61°17′ W 73°40′	3.44	1.4 ± 0.1
Brent, Ontario	Simple	N 46°5′ W 78°29′	3.8	396 ± 20[b]
Wanapitei, Ontario	Flat-floored (?)	N 46°45′ W 80°29′	7.5	37.2 ± 1
Deep Bay, Saskatchewan	Flat-floored	N 56°24′ W 102°59′	9.5[c]	99 ± 4
Nicholson Lake, NWT	Central peak	N 62°40′ W 102°41′	12.5	<400
Clearwater Lake East, Quebec	Central peak	N 56°5′ W 74°7′	20[c]	290 ± 20
Haughton, Nunavut	Central peak	N 75°22′ W 89°41′	24	23 ± 1
Mistastin Lake, Labrador	Central peak	N 55°53′ W 63°18′	28	36.4 ± 4
Slate Islands, Ontario	Central peak	N 48°40′ W 87°0′	30	~450
Clearwater Lake West, Quebec	Peak ring	N 56°13′ W 74°E13′	32[c]	290 ± 20
Carswell, Saskatchewan	Peak ring	N 58°27′ W 109°30′	39	115 ± 10[d]
Charlevoix, Quebec	Peak ring	N 47°32′ W 70°18′	54	342 ± 15[e]
Manicouagan, Quebec	Peak ring	N 51°23′ W 68°42′	80[c]	214 ± 1
Sudbury, Ontario	Multi-ring (?)	N 46°36′ W 81°11′	200[f]	1850 ± 3

[a]Data are from the Earth Impact Database (www.unb.ca/passe/ImpactDatabase.htm) except as noted.
[b]Radiometric age, as given, is too young, as an age of >452 Ma, i.e., probably Lower Ordovician, is indicated on stratigraphic grounds (Grahn and Ormö 1995).
[c]Diameter given here is based on diameter of residual gravity anomaly (see text).
[d]Alternatively, age may be Lower Paleozoic (365–515 Ma) (Bess 1985; Wanless et al. 1968), which is in better agreement with regional erosion history.
[e]Radiometric age, as given, is probably low (Whitehead 2003, personal communication).
[f]Diameter is based on distribution of shock features and limit of deformation in Huronian sedimentary rock.

Table 2. Other impact craters mentioned.[a]

Name	Morphological type	Location	Diameter (km)	Age (Myr)
Barringer, Arizona, USA	Simple	N 35°2′ W 111°1′	1.19	0.049 ± 0.003
Lonar, India	Simple	N 19°58′ E 76°31′	1.83	0.052 ± 0.006
Ries, Germany	Peak ring	N 48°53′ E 10°37′	24	15.1 ± 0.1
Boltysh, Ukraine	Central peak	N 48°45′ E 32°10′	24	65.17 ± 0.64
Puchezh-Katunki, Russia	Central peak	N 56°58′ E 43°43′	80	167 ± 3
Popigai, Russia	Multi-ring	N 71°39′ E 111°11′	100	35.7 ± 0.2
Chicxulub, Mexico	Multi-ring (?)	N 21°20′ W 89°30′	170	64.98 ± 0.05
Vredefort, South Africa	Multi-ring (?)	S 27°0′ E 27°30′	300	2023 ± 4

[a]Data are from the Earth Impact Database (www.unb.ca/passe/ImpactDatabase.htm).

fall back or fall out fragments, but for the most part, they are the fragmented or shock melted materials that, although mobilized, did not leave the crater but remained as a lining of the crater floor and walls. In some cases, the crater-lining sequence is preserved with little subsequent deformation. In others, there has been further disruption by late-stage movements. Where the allochthonous succession has not been disturbed, its lower contact is the fragmentation limit; beyond that limit, brecciation dies out except for relatively minor pockets of monomict breccia.

The rocks below the fragmentation limit may be displaced and deformed to varying extent but retain structural continuity. They constitute a parautochthone that, in turn, grades into rocks of the autochthone, country rocks that contain no evidence for substantial movement or internal change due to the impact event. As will be discussed, one of the main changes with crater size is the position of the limit of fragmentation relative to the extent of shock metamorphism. In this and other ways, the distribution of shock effects provides valuable data and raises important issues for consideration by modeling methods.

BACKGROUND

An attractive feature of studies of terrestrial impact structures from early days has been the attempt to marry theory, experiment, and observation. This has been fraught with difficulties and flawed assumptions, most famously illustrated by the pioneer efforts of Gilbert (1896) to reconcile evidence of meteorite impact at Meteor Crater, Arizona with an elementary understanding of impact mechanics. The vigorous debate in that arena over the next 60 years (Hoyt 1987) was mirrored elsewhere as enigmatic circular structures were recognized in many parts of the world, usually in stable regions where the rate of erosion has been low. The resolution of the Meteor Crater controversy, through the use of theory and nuclear explosion results (Bjork 1961; Shoemaker 1960, 1963), opened the way to the present consensus on the criteria for identifying impact structures (Dence 1972) and the current understanding of the impact record (Grieve 1998).

After the New Quebec and Brent craters where brought to the attention of scientists in 1951 (Meen 1950, 1957; Millman et al. 1960), C. S. Beals and colleagues at the Canadian Dominion Observatory began a systematic search for possible impact structures on the Canadian Shield (Beals et al. 1956). From the outset, they appreciated the importance of a sound theoretical basis for the interpretation of the morphologic and geophysical evidence that they amassed in the succeeding decade (Beals 1965). For a theory of impact, they turned to the pioneer work of von Neumann and Richtmeyer who used an early digital computer to follow the progress of a shock wave in a dissipative medium (Beals et al. 1963). A second major influence was the analysis by Baldwin (1949) of lunar craters in the light of data from experimental explosion craters. The simplified model that Beals and colleagues adopted combined crater profiles drawn from Baldwin with a substructure of concentric bowls of crushed breccia and fractured basement. This model was used in the interpretation of several craters examined in detail by geophysical methods followed by diamond drilling.

By 1960, it was apparent that the model was deficient in several ways. Baldwin's curve relating crater diameter and depth for bomb and lunar craters seemed to agree with the respective dimensions of Barringer, Holleford, New Quebec, and Brent craters (Beals et al. 1963; Millman et al. 1960). However, initial expectations that Deep Bay also fell on the curve had to be revised when drilling showed it to be considerably shallower than forecast (Innes et al. 1964). At that time the effect of gravity on crater form was not taken into account. On the other hand, there was an emerging realization from nuclear explosion data that the energy of hypervelocity impact is partitioned into heat and phase changes, as well as fracturing and ejection of both target and projectile. Innes (1961), for example, made allowance for the partitioning effect when he used density deficiencies from gravity surveys of Holleford, Brent, and Deep Bay craters to derive estimates of impact energy. His results lay within the broad range of energy estimates obtained by other methods but, by later calculations, underestimated the total energy involved (Dence et al. 1977).

Other difficulties reconciling observation with the impact hypothesis had arisen from early investigations of larger circular structures such as the Clearwater Lake West and Manicouagan craters (Beals et al. 1956). There were two unexpected features that seemed to be obstacles to an impact origin. One was the presence of large volumes of rocks of igneous texture that initially were taken by many investigators (Bostock 1969; Currie 1971; Kranck and Sinclair 1963) as flows of lava and, hence, evidence of a volcanic origin for the structure; some proposed impact-triggered volcanism. Subsequently, they have been accepted on structural, chemical, and isotopic grounds as the products of impact melting (Dence 1971; Floran et al. 1978; Grieve 1978; Grieve et al. 1977). A second puzzling feature, for which a complete explanation remains more elusive, was the presence of a central peak and evidence from gravity and seismic profiles (Sweeney 1978; Willmore 1963) that the center was not strongly fractured, unlike smaller craters. As a result, it was not until shock metamorphism was fully accepted as an unambiguous criterion for hypervelocity impact (French and Short 1968, and papers therein) that the impact status of these craters was confirmed.

SHOCK METAMORPHISM AS A STRUCTURAL TOOL

Soon after the acceptance of natural shock metamorphism as the prime criterion of hypervelocity impact, it became evident that the distribution of shock features could be used to elucidate the mechanics of impact crater formation. An important early demonstration was the use of shatter cone orientations (Dietz 1968; Manton 1965) to determine the net inward and upward displacements involved in the formation of central peaks in stratified sedimentary successions. Restoring the rocks to their original positions demonstrates that the shock wave originated near the surface, indicates their net trajectories during uplift, and outlines the parabolic profile of the transient crater formed during the early excavation stage before the uplift of the center (Dence et al. 1977). Obtaining comparable structural information for craters formed in crystalline rocks is less direct and requires a careful mapping of the levels of shock metamorphism in indicator minerals, of which quartz and feldspar are the most important.

The detailed study of shocked rocks and minerals in terrestrial settings began with studies of ejecta at Meteor Crater (Chao 1968), inclusions in suevite at the Ries (Stöffler 1966; von Engelhart and Stöffler 1968), and shock effects resulting from nuclear explosions (Short 1968). Applying those results to older Canadian structures was hindered, in part, by the obscuring effects of deep erosion and alteration. On the other hand, besides shatter cones, melt rocks resulting from shock pressures exceeding 60 GPa and planar deformation features (PDFs) in quartz and feldspar, produced in the 5–25 GPa range of shock pressures, are commonly well-preserved, even in craters of early Paleozoic age or older. In addition, the continuous diamond drill core obtained from several craters provided details of the distribution of shocked materials to depths of as much as 1 km.

The extensively drilled Brent crater became the prime arena for using shock metamorphism to understand crater relationships and mechanics. The recovered cores included sequences of strongly mixed breccias, sections of shock melted material, and deeper intervals where relatively undisturbed, moderately to weakly shocked rocks showed progressive diminution of shock with depth (Dence 1968). Shock effects range from total melting indicative of the highest pressures to progressively weaker developments of planar deformation features in quartz, feldspar, and other minerals, as described by Robertson et al. (1968). The analysis revealed that the subsurface structure of craters of simple form is more complex than had previously been recognized (Beals et al. 1963; Dence 1965) and indicated that late-stage redistribution of shocked rocks is substantial.

A classification by zones was adopted (Dence 1968) as a means of mapping the intensity of shock metamorphism. This was later augmented by a more quantitative approach (Dence et al. 1977) that used detailed measurements of planar deformation features (PDFs) in quartz and, to a lesser extent, feldspar. The calibration based on laboratory data (Hörz 1968) recognized the variable development of shock deformation within large rock masses. For example, at the Mont de Babel anorthosite massif that forms part of the central uplift at Manicouagan crater, the author observed maskelynite as localized concentrations up to centimeters across that grade into plagioclase of near-normal birefringence over a few millimeters, or even within single grains. Similarly, quartz commonly shows variable development of PDFs both within and between grains (Robertson et al. 1968). To capture the range of variation within a sample, Robertson measured some 25 or more grains of quartz per thin section, assigning a nominal shock pressure to each grain according to the observed PDF orientations and other optical properties. From these data, an estimated mean shock pressure was calculated for each sample. The method was applied to analyze shock zones at Brent and two other craters, Slate Islands and Charlevoix (Grieve and Robertson 1976; Robertson 1975).

Several factors, yet to be thoroughly evaluated, introduce some uncertainty into such calculations. Robertson and Grieve (1977) have drawn attention to the effect of grain size specifically in cases such as the Slate Islands structure where quartz grains are smaller than the millimeter scale of typical granitic rocks in the Shield. Likewise, the author has observed coarse crystals of quartz in pegmatite veins at Charlevoix that show stronger development of PDFs than quartz in adjacent medium grained gneisses. Relative abundance is a second factor, as minerals present as minor constituents may show less evidence of shock damage than the dominant phases that form the framework of the rock and, therefore, take the brunt of the shock-induced deformation. For example, from personal observation, mica and other minor phases within maskelynite may show no visible deformation as may small feldspar inclusions within dark minerals.

The tabular data of Robertson (1975) show that the range of shock pressures expressed grain by grain in representative granitic rocks is on the order of ±5 GPa. By taking an average, the pressure assigned may be somewhat lower than a value based simply on the first appearance of particular shock features but is arguably more representative of the mean pressure pulse. The pressure calculated is taken to the nearest GPa, not to imply high absolute precision but to indicate differences in shock pressure between nearby samples in continuous rock sequences. The overall consistency of the results at the three craters examined in this way (Grieve et al. 1977; Robertson and Grieve 1977) gives confidence that they are useful in making estimates of apparent gradients of shock pressure for structural analysis.

Shatter cones are generally considered to be the direct consequence of the passage of shock waves and their reflections. They commonly occur in the zone where the pressure pulse consists of an elastic precursor followed by a plastic wave (Dietz 1968; Milton 1977). A complete theory of shatter cone development has yet to be formulated, but it is generally accepted that they form early in the cycle of shock loading and unloading and so provide an indication of the differential stresses related to the passage of the shock. The matter of the timing of shatter cone fracturing relative to the fragmentation that produces breccias at the transient cavity stage is an open question. Virtually all known shatter cone occurrences are found in central uplifts and so are in rocks of the parautochthone beyond the limit of fragmentation. This is the case at Charlevoix, where the relationship of shatter cones to mineralogical shock features is well-displayed (Robertson 1975), as discussed below.

STRUCTURAL ANALYSIS OF SIMPLE CRATERS

General Characteristics

While Meteor Crater, Arizona, is the largest simple crater formed in sedimentary rocks and is the acknowledged model of crater mechanics (Roddy 1977; Shoemaker 1960, 1963), it is well known that others formed in crystalline target materials have diameters up to 4 km. Lonar Lake, India (Fredriksson et al. 1973) and craters within this range in Scandinavia (Abels et al. 2002) and elsewhere, provide valuable information on the general subsurface configuration of breccias in craters that lack central uplifts. In Canada, the well-preserved New Quebec crater furnishes important data on rim structure and other aspects of the surface expression of such craters, while subsurface information has been obtained from three others by diamond drilling. Of the latter, the two smaller, Holleford (Beals 1960) and West Hawk Lake (Halliday and Griffin 1967; Short 1970), exemplify craters formed, respectively, in Grenville Province marbles and other metasediments and Superior Province greenstones. However, the extensive drilling at the 3.8 km Brent crater, Ontario (Fig. 1) has yielded the most complete picture of the anatomy of a simple impact crater and is the main source of insights into the mechanics of crater formation in crystalline rocks. The elements of greatest interest in this respect are the nature and distribution of breccias and melt rocks, the level of shock metamorphism in both breccias and underlying basement rocks, and evidence for shearing and relative motion within and at the base of the breccia lens.

Breccias and Melt Rocks

As outlined above, the initial impression from drilling at Brent in 1955, 1959, and 1960 was of a sequence of breccias below the sedimentary cover within the crater, underlain by fractured but relatively undisturbed country rocks (Beals et al. 1963). This was clearly colored by the prevailing model at the time and missed the significance of a layer of igneous rocks encountered at a depth of about 1 km, interpreting them as a pre-existing sill. Petrographic examination showed that the igneous rocks were different from pre-impact dikes found in the region including alnöites, dated as latest Proterozoic or Cambrian (Hartung et al. 1971), that do occur in the rim rocks of the crater and are a minor component of the Brent breccias. Interpretation of the igneous layer as a lens of impact melt (Dence 1968, 1971) was reinforced by the results of drilling in 1967 and detailed analysis (Dence and Guy-Bray 1972).

Depicting the complexities of the breccias and other relationships at Brent has proved difficult. Presentations have not been completely consistent (e.g., Dence 1964, 1965, 1968, 2002; Dence et al. 1977; Dence and Guy-Bray 1972; Grieve 1978; Grieve and Garvin 1984; Grieve et al. 1981; Hartung et al. 1971), reflecting, in part, changes in ideas and emphasis. Certain features have assumed greater importance as observations are compared with evolving impact theory. Following the recognition of the melt rocks as an integral part of the crater sequence, the main changes in interpretation have arisen from the realization that shock effects do not diminish regularly with depth but wax and wane with little apparent regularity, except near the base. In the drill holes within 1 km of the center, one or two layers of melt plus mixed breccia resembling suevite are found in the upper approximately 100 m of the breccia mass (Fig. 1). Otherwise, except in the center, the bulk of the breccias are only slightly mixed and weakly shocked. In addition, drill-holes B1-59 at the center and B1-67, 200 m away demonstrate that the melt rocks at depth are constrained to a circular lenticular form, the upper surface horizontal and the lower concave, about 200 m in radius and 42 m thick at the center. It is now generally accepted that it represents the limit of penetration of shock melted target rocks mixed with remnants of the projectile (Dence 1968; Grieve 1978; Palme et al. 1981).

In the resulting reappraisal of the structure of the crater in the light of these results, it became evident that a two-stage

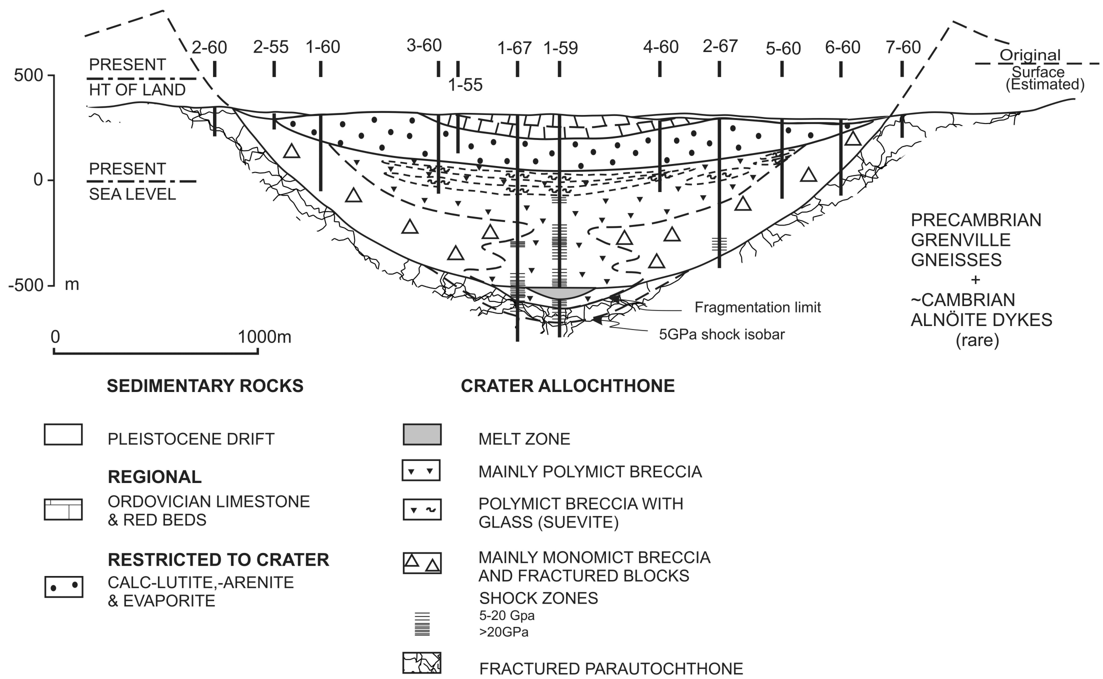

Fig. 1. Brent crater cross-section. Projection onto a diameter of the present crater profile and its reconstruction before erosion, showing drill holes, distribution of post-impact sedimentary rocks (lower units being restricted to the crater, upper units being fossil-bearing regional rocks), brecciated rocks, melt-rich layers, and zones of shock metamorphism. The limit of fragmentation is cut by the primary shear, the lowermost of the shears along which slabs of the crater wall have moved to create the final crater fill (additional shears are shown in Fig. 5b). Breccias at depth in the center, below the primary shear and the lens of melt rocks, are not disturbed by late-stage slumping and, as relicts of the transient crater, are used to estimate net displacements down axis (Dence 1968; Dence and Guy-Bray 1972).

crater-forming process was required. The revised interpretation (Dence et al. 1977) incorporated, as a first stage, the formation of a deep, approximately paraboloid, transient crater, with walls dipping at an average slope of about 35°. The floor and walls are lined with an allochthonous layer about 80 m thick in the center comprising shock melt overlying mixed breccias of displaced but not ejected material. The second stage was conceived as an immediate collapse of the walls of the transient cavity. It resulted in an inter-layering of strongly shocked and mixed material from the transient crater lining and weakly shocked, partially brecciated and only slightly mixed rocks derived from the parautochthonous basement rocks of the transient crater walls (Fig. 1).

There are additional features that are largely confined to the 600 m-thick axial region as seen in drill core from B1-59 and, in part, B1-67. As in other holes, two melt-bearing, mixed breccia layers were penetrated in the upper 140 m of the crater sequence below the sedimentary fill. However, the central section at this depth is distinctive in that the matrix, as well as strongly shocked clasts, is locally vesicular (Beals et al. 1963), suggesting further heating and degassing of already shocked and crushed rock. A possible explanation is that additional heating resulted from the violent collision of material sliding rapidly from the walls of the collapsing transient cavity. This zone is underlain by moderately mixed breccias about 260 m thick in which shock levels average about 15–20 GPa. Then there is a 50 m-thick interval of weakly shocked, coarse, slightly mixed breccias underlain by a 110 m interval in which fragmentation and mixing is more pronounced. With increasing depth, shock levels rise progressively, but toward the bottom of this section, shock effects are overprinted by thermal recrystallization as a result of proximity to the underlying impact melt rock (Dence 1968; Grieve 1978). The latter consists of a fine-grained, amygdaloidal matrix with conspicuous recrystallized clasts in the upper 10 m, a coarser grained 15 m-thick central section with few clasts, and a 17 m-thick lower zone of finer grain size in which partly digested clasts are again conspicuous. The analysis of the melt shows it to be a mix of the country rocks with the addition of about 1% chondritic meteorite (Palme et al. 1981). Beneath the melt is a section of breccia about 80 m thick of which the upper 20 m are thermally recrystallized (Fig. 2). In the remaining brecciated section, where the rocks retain their primary minerals, and in the underlying parautochthone, steadily decreasing shock levels have been mapped (Dence 1968; Robertson and Grieve 1977). The shock zones thereby recorded are surprisingly narrow and imply a strikingly rapid attenuation of shock pressure. Understanding this result has been fruitful in unraveling the sequence of events at Brent and, by extension, at other simple craters (Dence 1968, 2002; Dence et al. 1977; Robertson and Grieve 1977).

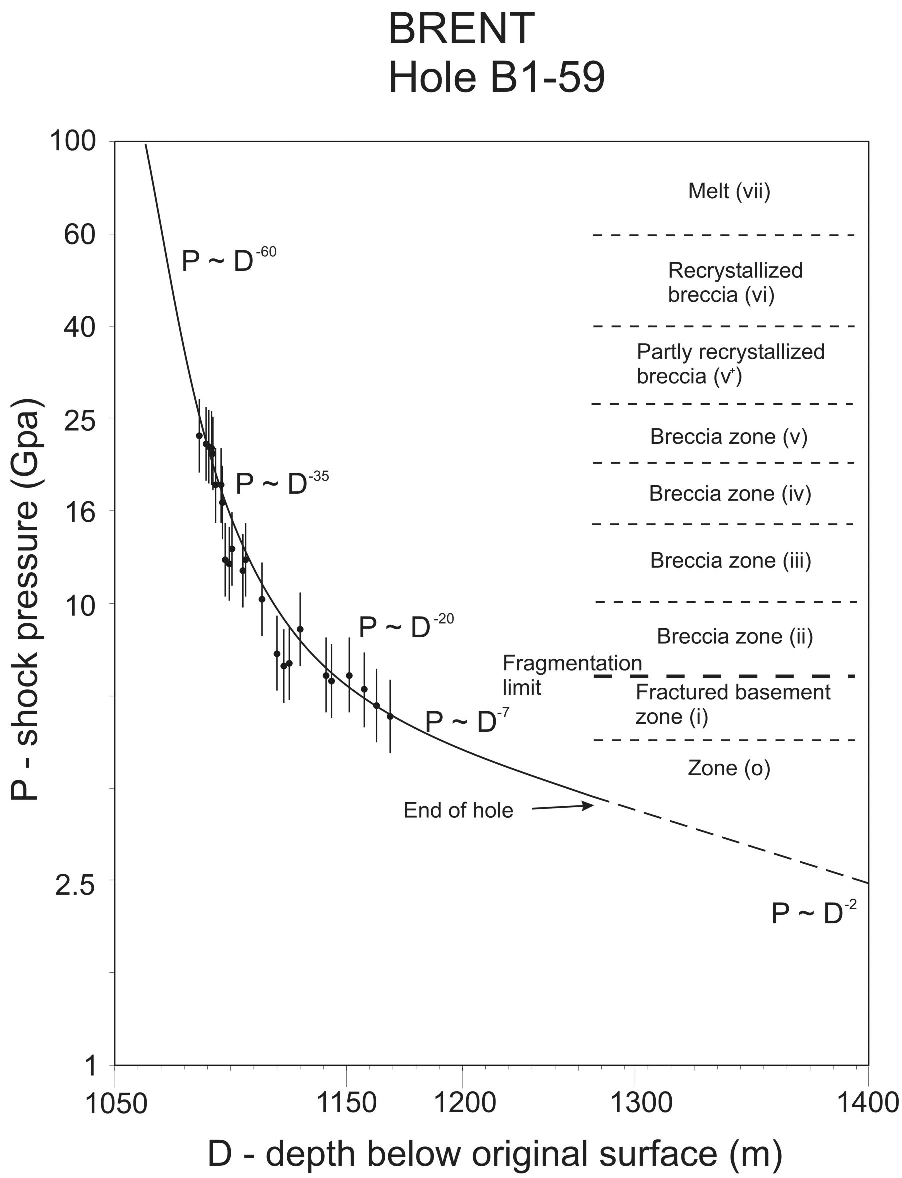

Fig. 2. Brent central drill-hole (B1-59). Log-log plot of mean shock pressure (GPa) below the melt zone versus depth below the original surface. A calibration of breccia zones and representative values of the exponent of apparent attenuation are indicated at various depths (after Dence 1968, 2002; Robertson and Grieve 1977).

Shock Attenuation and Crater Mechanics

The compaction of shock zones at Brent, mentioned above, and also at West Hawk Lake crater (Short 1970) resemble those observed beneath craters formed by hypervelocity impact experiments using layered non-cohesive quartz sand targets (Gault et al. 1968). However, the difference in target materials introduces uncertainty as to how applicable this analogy is to natural craters formed in crystalline rock. The situation is clarified by important data from the buried Piledriver nuclear explosion, a 61 ± 10 kt (TNT equivalent) test in Climax granodiorite at the Nevada Test Site. Various gauges for which the pre- and post-shot positions are known measured pressures up to 27 GPa (Borg 1972). The results (Fig. 3) demonstrate compaction of shock zones around the shot point similar to that observed below the melt rocks at Brent. Restoring the gauges to their original positions shows that, in this medium, shock pressure (P) attenuates over the range measured as P ~ R^{-2}, where R is the distance from the shot point. There was some uncertainty in applying this result to Brent (Dence et al. 1977) as it seemed possible that the rate of attenuation may change with scale in some unforeseen fashion. Indeed, in that study, a range of possible rates was considered. An exponent of –2.5 was favored as the –2 value seemed to require the final crater to be too large relative to the calculated energy and the volume

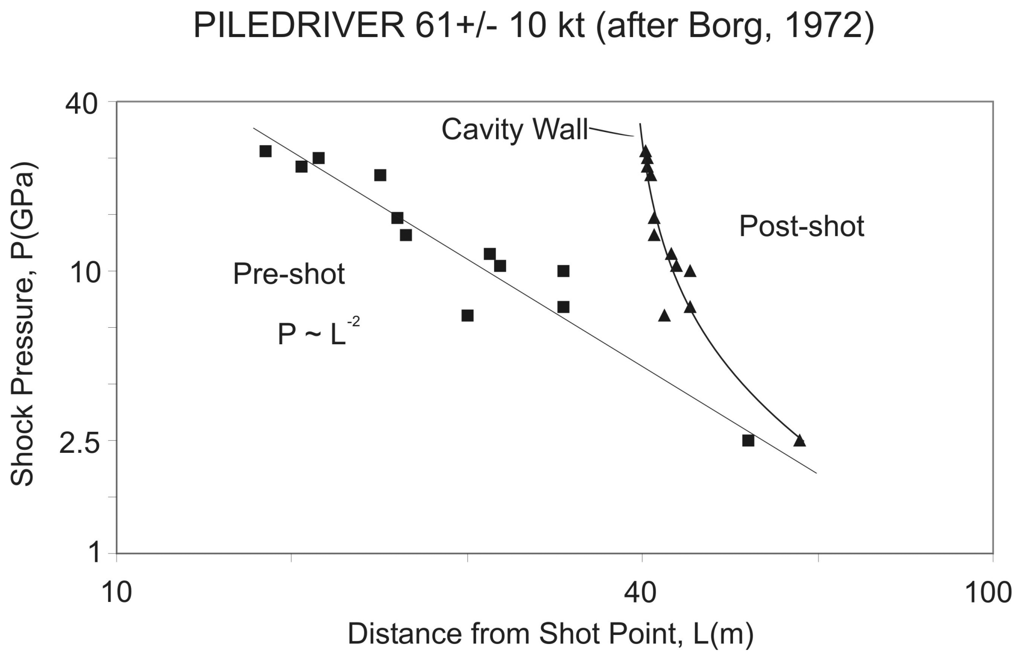

Fig. 3. Piledriver underground nuclear test in Nevada granodiorite. Pre- and post-shot positions of shock pressure gauges indicating actual attenuation of P ~ L^{-2} (after Borg 1972).

excavated when compared with craters formed experimentally by nuclear and other explosives.

A resolution of this question comes from a second source, namely the analysis of shock pressure attenuation by Ahrens and O'Keefe (1977) through computer modeling using equation-of-state data for lunar gabbroic anorthosite (Fig. 4). Their results have been applied to the analysis of feldspar-rich, high-grade gneisses at Brent on the assumption that differences in physical properties are not significant. Likewise, the computations treat dissipation of shock pressure down axis from a vertical impact. The Brent central drill hole data are down axis, and the close approximation to circular symmetry that the crater exhibits in plan and cross-section suggests that deviation of the angle of impact from vertical was similarly not significant.

The Ahrens and O'Keefe analysis illuminates a key factor that was not considered previously as it was not measurable at the Piledriver test, namely the distinction between near and far fields. Their results for attenuation in the far field, within a range in projectile composition and velocity, are similar to those measured in the Piledriver nuclear event. However, the calculated rate of shock pressure attenuation for the near field, within about 2.5 projectile diameters of the impact point, is only ~–0.2. By accepting similar rates for the near and far fields at Brent, reasonable results are obtained for the energy release by that impact. To compare the Brent data with their calculation, an estimate must be made of the down axis depth where the observed rate of attenuation converges on the nominal rate of P ~ R^{-2}. For a stony projectile impacting at 15 km/s, Dence (2002) estimated the convergence depth to be 1,220 m below the original surface where the shock pressure had dropped to about 5 GPa. At this depth, about 75 m below the lower limit of fragmentation, the rock is virtually unchanged from normal country rock.

Displacements down axis of material shocked to specific shock grades can be derived from the model (Fig. 4) and the distortion normal to the axis estimated from the apparent attenuation rate. For example, a disk of the target rock originally located just below the zone of complete shock melting is calculated to have been displaced downward about 735 m and was spread laterally, as breccia, across the crater floor until about 5–6 times its original radial extent. The Ahrens and O'Keefe results are normalized to the radius of the projectile, so a nominal size for the bolide that formed the Brent crater can be calculated (diameter ~110 m) and a corresponding energy of impact (3×10^{17} J) derived (Dence 2002). These results are comparable to those estimated in earlier studies.

Shear Zones

Further examination of the Brent cores has brought an additional feature to prominence: the presence of thin shear zones within and below the breccias. The zones are typically from a few centimeters to some meters thick and include fine-grained breccia that, in some cases near the margin of the breccias, were first interpreted as thin lenses of impact melt (Dence 1965, 1968) but are reinterpreted here as altered frictional melt. Such zones are most abundant in the center but are more clearly visible in hole B2-67, midway between the crater center and its margin. At this distance, the mass of

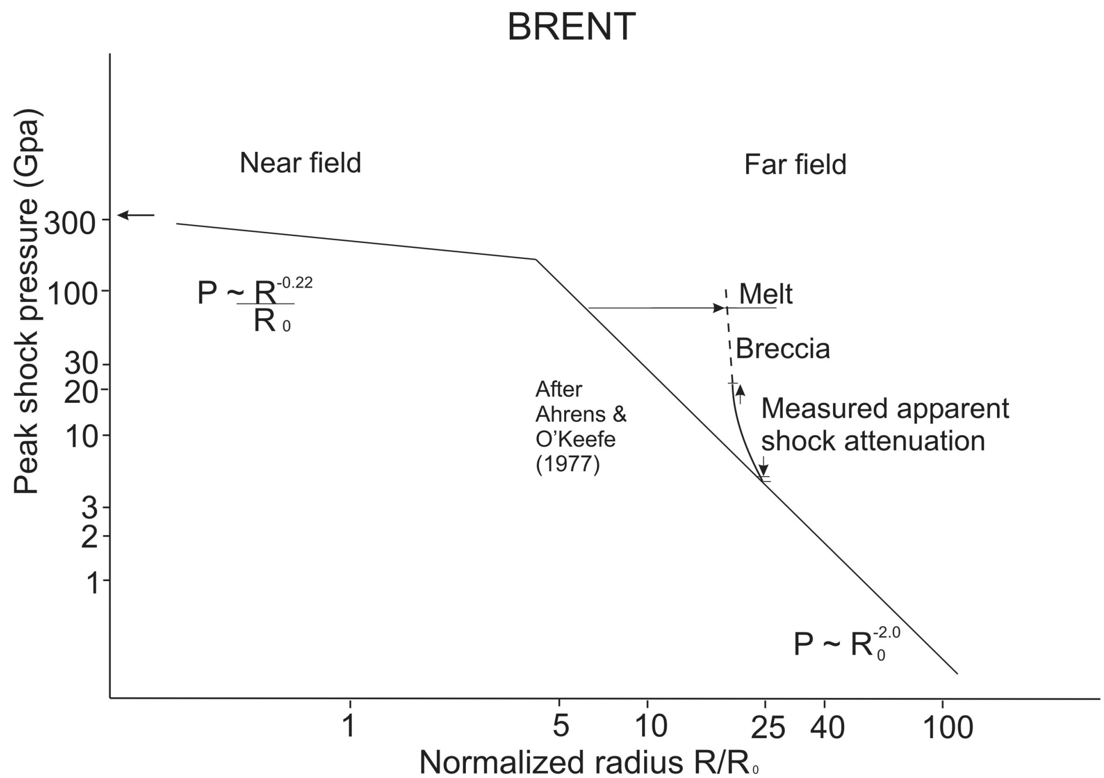

Fig. 4. Comparison of apparent shock pressure attenuation at Brent crater with generalized model for a stony bolide with velocity of 15 km/s (Ahrens and O'Keefe 1977). The curves merge where observed and actual attenuation rates are similar at ~5 GPa shock pressure. This enables calculation of displacements (e.g., limit of shock melting taken as 60 GPa) and provides a size of bolide and, hence, impact energy (see Dence 2002).

displaced rock is about 500 m thick, but only the upper half is strongly brecciated. Midway down the crater sequence, the drill hole intersects a shear zone that is the approximate lower limit of distinct brecciation. Locally brecciated, slightly mixed rocks occur at greater depth terminating at a second shear zone some 180 m deeper. In some representations of the cross-section of the crater, this zone is depicted as the base of the breccias. However, about 100 m below the second shear, there is a third in otherwise mildly fractured rock. Clearly, displacement has occurred on this zone as it marks a change from rock with no evidence of shock metamorphism above the zone to rock with distinct, though weak, shock features below. The shears are here interpreted as planes along which sheets of rock on the order of 100 m thick have slid from the crater walls toward the center. It may be inferred that additional fragmentation and mixing occurs in the center where the sheets collide. Likewise, the largely monomict breccias intersected by holes B1-60 and B6-60 near the margins result from the disintegration of the trailing edges of the sheets, thereby adding to the total volume of breccia.

For the most part, the shears cannot be traced from one hole to the next. However, a surface defining the base of the entire displaced mass within the crater can be traced from the crater margin at the present surface to the center of the melt rock zone in B1-59. At the margin, it is expressed as a topographic notch marking an abrupt change of slope from the low-lying crater fill to the parautochthonous rocks that underlay the original rim. In plan view, the notch is nearly perfectly circular. Its nature is not clear at the surface as subsequent sedimentary rocks and glacial drift hide the trace of the boundary at the present level of erosion (Dence and Guy-Bray 1972). In cross section, the surface passes, in turn, through the lower limit of breccias in B6-60, the lowermost shear zone in B2-67 and the margin of the thermal aureole due to the melt rocks in B1-67. Previously, it has not been recognized that the surface, so defined, closely approximates a segment of a sphere with radius about twice the depth to the center of melt zone. There is no indication that changes in lithology, rock texture, gneissosity, or pre-existing structures in the country rocks have any significant effect on the shape of this spheroidal surface. These characteristics suggest that it is a superfault, in the terminology of Spray (1997). Here, it is identified as the primary shear (Fig. 5) with radius $r_s \approx 2d_t$, where d_t is the depth of the floor of the transient crater from the original surface (estimated to be about 70 m above the present height of land in the vicinity of the crater). The interpretation favored here is that the shear controlled the collapse of the crater walls and was superimposed on the existing rocks in response to the stress field in effect as the transient cavity reached or began to relax from its maximum size.

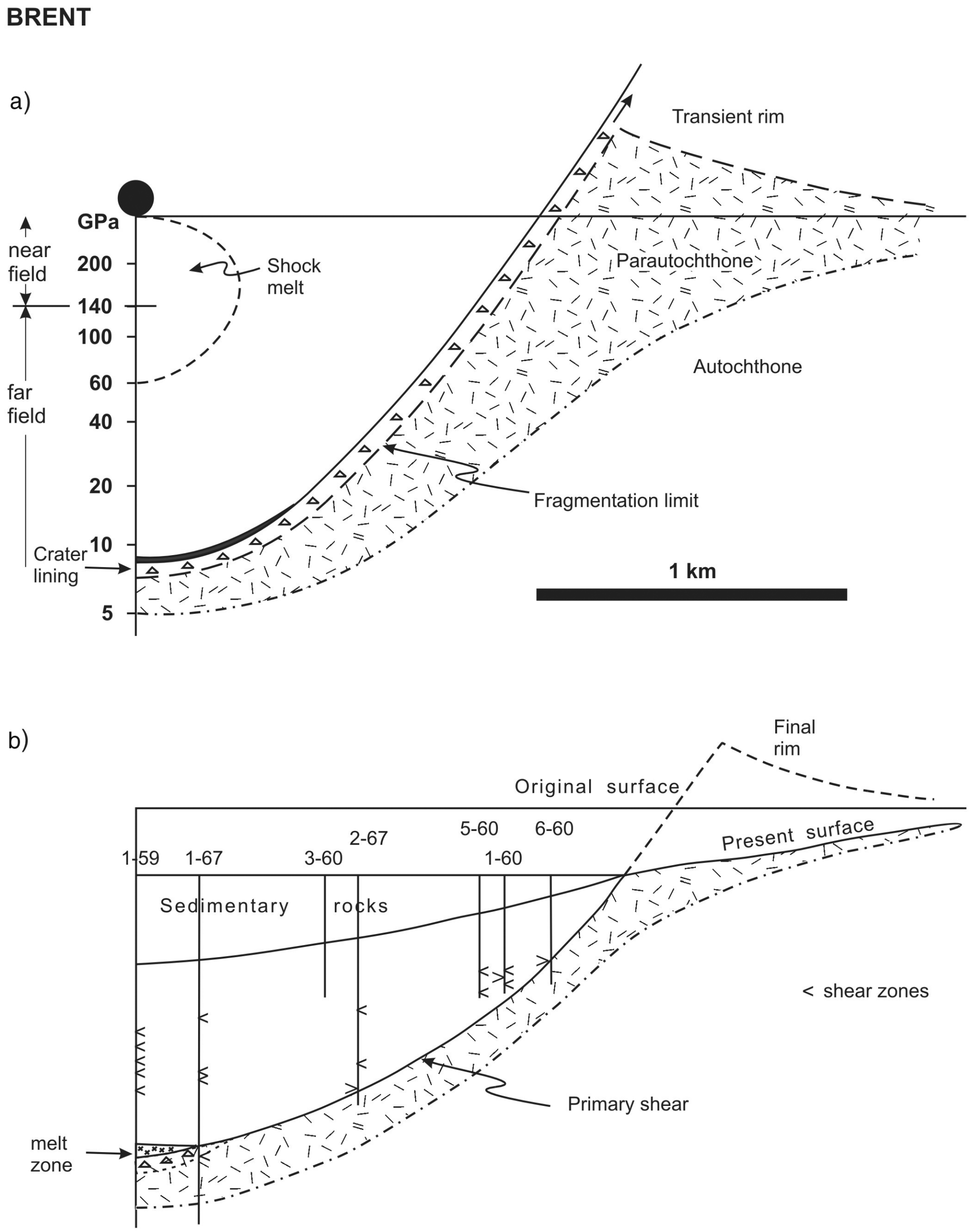

Fig. 5. Brent crater. Reconstruction of the transient and present crater profiles. In (a), actual shock pressure is shown down axis along with the transition from near- to far-field, the volume melted by shock, and the size of a nominal stony bolide (vertical impact at 15 km/s). The transient crater boundary corresponds to the fragmentation limit, overlain by a lining up to 80 m thick of mixed breccia and impact melt. The lining is underlain by a parautochthone of locally fractured and brecciated country rocks, grading into an undisturbed autochthone; the short-term displacement due to elastic compression is not depicted. In (b), the primary shear bounds the lens of displaced breccia fill. The shear corresponds to a sphere segment with radius $r_s \approx 2d_t$, where d_t is the depth from the impact point at the original surface to the mid level of the melt zone; additional shears within the breccia fill are also indicated (data sources are as for Fig.1).

COMPLEX CRATERS

Considerations in the Structural Analysis of Complex Craters

The methods used to analyze simple craters must be adapted to the different features of complex craters. A calculation of impact energy cannot be made in the same direct way, so an expression relating crater diameter and energy is required. Cooper (1977) and others have noted that, where the medium does not change, the size of craters formed by large nuclear explosions scales according to $D \sim E^x$, where D is the final diameter of the crater, E is the energy, and $x = 1/3.4$, i.e., 0.294. This value for the exponent lies between pure energy scaling (x = 1/3) and gravity scaling (x = 1/4) and has been taken, in such cases, as an estimate of the relative importance of the two factors. By analogy with nuclear explosions, x = 1/3.4 has been used to calculate the energy of formation of large impact structures (e.g., Dence et al. 1977). With the energy for Brent given above, the expression derived is:

$$D = 2.75 \times 10^{-5} E^{1/3.4}$$

(Dence 2002), where *D* is in kilometers and *E* in joules. The formula gives a calculated energy for Charlevoix of 2.5 × 10^{21} J. Although that result is used here for the purpose of illustration, it is quite likely that, with increasing size, the exponent tends toward gravity scaling (Gault et al. 1975). In that case, the energy calculated for Charlevoix would be greater, and the expression would require additional adjustment.

An additional reason that the model for simple craters outlined in the preceding section cannot be applied directly to craters with a central peak is lack of information down the central axis. In most cases, depth of origin cannot be estimated with any accuracy for crystalline rocks of the Canadian Shield. Further, by analogy with structures where the uplifted rocks are sedimentary, the critical section that, at Brent, lies below the melt zone is disrupted and tilted during uplift. The degree by which the rocks of the central uplift in complex craters have been distorted usually cannot be determined directly, but it is probable that they have been strongly tilted and broken into large blocks. Drilling results at complex craters of intermediate size, such as Deep Bay and the two at Clearwater Lake support this inference. Crystalline rock cores from near the centers of these three craters show only gradual decline from moderate to weak shock metamorphism over depths of hundreds of meters (Dence et al. 1977), thereby suggesting that the vertical drill holes intersect the shock zones obliquely at steep angles. The rocks are locally crushed and sheared and have fracture porosity similar to that of associated allochthonous breccias (Dence 1965; Dence et al. 1965).

However, the central peaks of larger craters show little sign of fracturing and crushing at the mesoscopic scale. Rocks of the central uplift at Charlevoix and other large craters must have moved as massive blocks separated by relatively thin shear zones that are rarely observed in outcrop. A comparable example is that of Puchezh-Katunki (Ivanov et al. 1996). At the largest of the well-preserved Canadian craters, Manicouagan, the rocks of the anorthositic part of the central peak lying above the tree line are clearly exposed over distances of kilometers. Layers of mafic minerals (mainly garnet and pyroxene) can be traced for hundreds of meters or more with only minor offsets. More documentation is needed, but a preliminary view is that blocks increase in size with crater size and that, in the larger craters, shears and fractures are more strongly developed toward the margins of the central uplifts than in the center.

Gravity results confirm that there is little fracture porosity in the rocks of the central peaks of craters >30 km (Sweeney 1978). On the other hand, pseudotachylite veins are increasingly conspicuous with crater size but rare in craters <30 km across. Spray (1998) has discussed the types and genesis of pseudotachylites found in the largest impact structures. Dence (2002) drew the inference that, in craters >30 km in diameter, the rocks of the central peak dilate as they rise, allowing the injection of friction melt and fine breccia from shear zones. On subsiding to their present positions, much of the porosity that may have been created is sealed by the injected veins.

Shock Metamorphism in Parautochthonous Rocks

A complementary data set to the down axis data in simple craters is obtained from surface sampling at complex craters where there is good exposure of the parautochthone. The prime example from the Canadian craters is the 54 km-diameter Charlevoix crater in Quebec (Fig. 6), where, with minor exceptions, all breccias and melt rocks have been removed by erosion. Rocks exposed at the present-day surface are mainly moderately to weakly shocked charnockites and anorthosites, the dominant rock types of the Grenville Province in the region (Rondot 1989). The present topographic relief mirrors the crater morphology, though extrapolation from less eroded craters indicates that on the order of 500 m of crater fill has been removed since formation. There is a well-developed central massif, Mont des Éboulements, that is surrounded by a ring of subdued hills and a peripheral trough within which discontinuous exposures of pre-impact lower Paleozoic limestones and other sediments are preserved (Rondot 1968, 1989). On the eastern side, the crater is almost bisected by the St. Lawrence fault and Logan's Line, a thrust that marks the western edge of the Appalachian Mountain system.

Shock metamorphism of the parautochthone at Charlevoix (Robertson 1968, 1975) is zoned concentrically, with the most strongly shocked rocks at the crest of the central peak, decreasing radially toward the margin. To the east of the St. Lawrence fault, it is evident that the shock zones have been perturbed by post-impact tectonic disturbance. Data from this part of the structure are omitted from this discussion. Robertson (1975) and Robertson and Grieve (1977) interpreted the main distribution of shock zones in terms of uplift of the center of the transient crater. However, they found that the model for their reconstruction of the transient crater that provided the best fit to the data required the rate of shock pressure attenuation to be as $P \sim R^{-4.5}$.

Omitting tectonically disturbed data east of the St. Lawrence fault, a log-log plot of observed shock pressure projected onto a radius (Fig. 7) shows that the rate of apparent attenuation is low near the center, averaging about $P \sim R^{-0.3}$. Shock levels drop from about 23 GPa at the center to about 5 GPa, the lower limit of PDF development in quartz, about

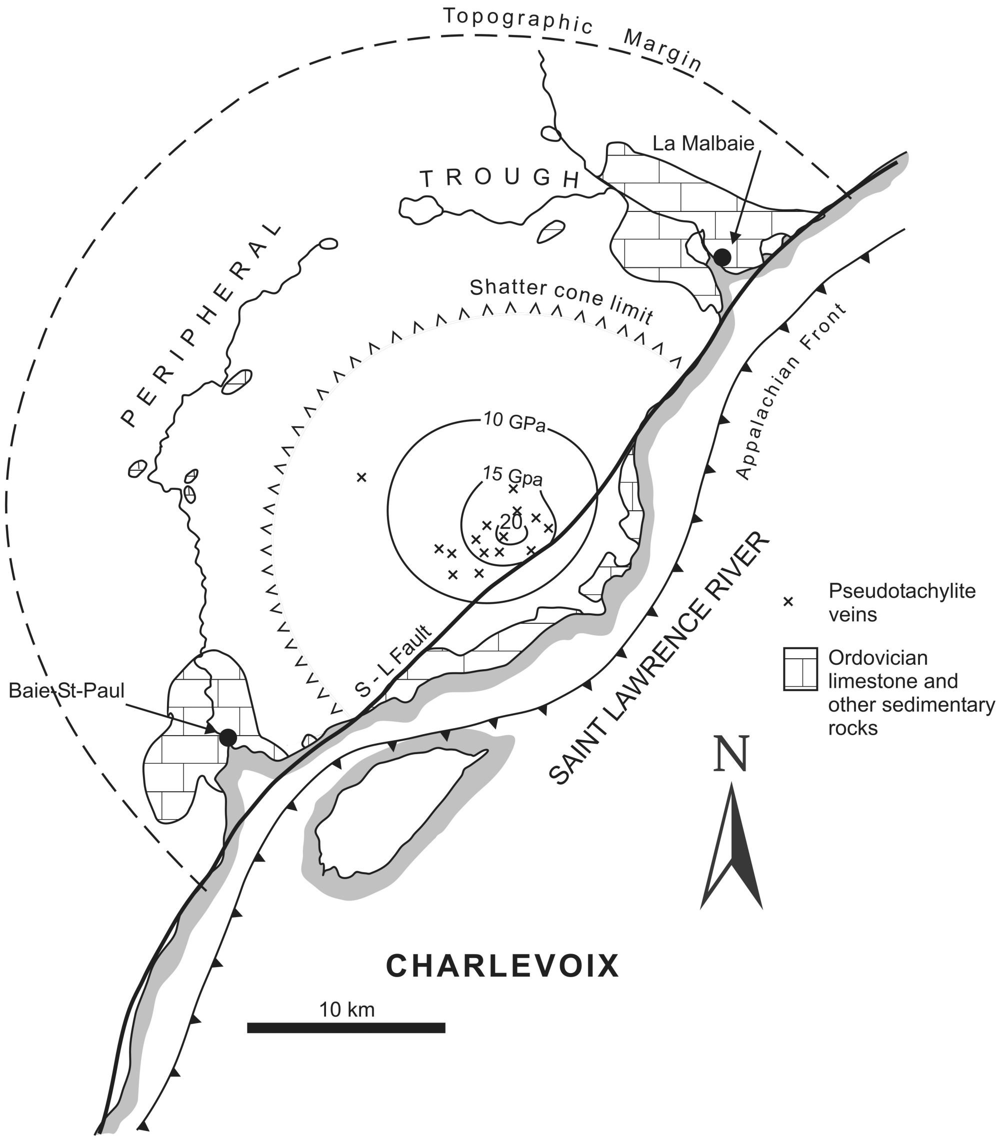

Fig. 6. Charlevoix crater. Simplified map showing shock isobars, distribution of shattercones and pseudotachylites, and main topographic and structural features (modified after Robertson 1975; Rondot 1989). The topographic central peak corresponds closely to the 20 GPa isobar. The peripheral trough is a topographic low underlain by down-dropped, strongly faulted and folded pre-impact lower Paleozoic sedimentary rocks. The rim is defined by the margin of a regional plateau with average elevation about 900 m above the river. The Appalachian Front (Logan's line) is the trace of a thrust dipping 20° SE; the St. Lawrence (S-L) fault is a zone of late (still active) normal faulting.

half way to the axis of the peripheral trough (Robertson 1975). From that point to the margin, shock pressure estimates are based largely on shatter cone development. Most shatter cones at Charlevoix are in coarse-grained rocks and so are relatively crude compared with their archetypical appearance in fine-grained rocks. They have not been recorded in the rocks of the central peak that experienced shock pressures >20 GPa but occur in an annular zone from about 3 km to 12–14 km from the center. This corresponds to rocks shocked to between 15–20 GPa to those beyond the limit of PDF development in quartz at 5 GPa. The pressure at the shatter cone limit is estimated as ~2 GPa. The most abundant and well-defined cones occur near the 10 GPa isobar. The data from the outermost quartz and shatter cone occurrences suggest that rate of apparent shock attenuation in this part of the crater is about $P \sim R^{-3}$. The change in slope at about 9 km from the center corresponds to the hinge region between the inner zone that has been uplifted to form the central peak and the margin that has dropped. Down faulting at the periphery is confirmed by the preservation of pre-impact, near-surface sedimentary rocks in the peripheral trough.

For an alternative reconstruction of the transient cavity for Charlevoix (Fig. 8), it is assumed that the down axis attenuation of shock pressure is $P \sim R^{-2}$, as at Brent. The isobars delineating the imprint of shock pressure at depth are taken to have been hemispherical with center near surface,

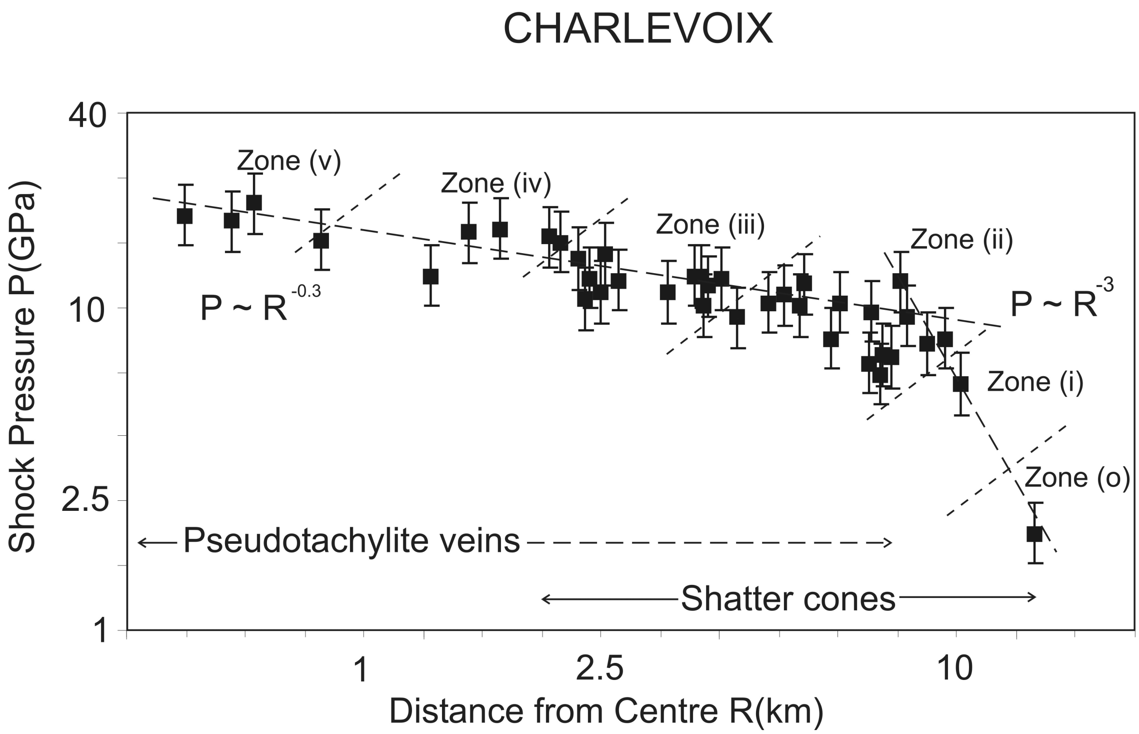

Fig. 7. Charlevoix. Log-log plot of mean shock pressure versus radial distance from the center at the present surface with tectonically disturbed sites lying southeast of the St. Lawrence fault omitted (Robertson 1968, 1975; Robertson and Grieve 1977). Shattercones occur in a zone between the 15 and 2 GPa isobars. Pseudotachylite veins up to 2 cm thick are largely confined to rocks <3 km from the center, with thin veins to a radial distance of 9 km. The apparent average rate of shock pressure attenuation is $P \sim R^{-0.3}$ within about 8 km of the center, changing to $P \sim R^{-3}$ at the hinge between the uplifted center and the down-dropped margin.

approximately one bolide diameter below the point of impact. The observed maximum shock level at the central peak, with allowance for some loss due to erosion, provides an estimate of ~25 GPa for the down axis fragmentation limit. It is further assumed that the net trajectories of the parautochthone during uplift was similar to that deduced at Gosses Bluff and similar craters formed in sedimentary rocks (Dence et al. 1977), based on shattercone orientations and observed displacements vertically and toward the center (Milton et al. 1996). To match the observed radial distribution at the present surface, the transient crater outline must cut the isobars obliquely at depth. These conditions are satisfied if the profile of the transient crater is approximately parabolic. Near the surface, the fit becomes less satisfactory but improves if the shock isobars tighten so that the actual attenuation in that region approximates $P \sim R^{-3}$, in agreement with the interpretation of the data (Fig.7). This accords with Melosh (1989) who pointed out that shock pressure will attenuate more rapidly in the near-surface regime than down axis.

The resultant transient crater resembles that derived for simple craters and complex craters formed in sedimentary rocks (Grieve et al. 1981). The presence of a topographic ring around the central peak at Charlevoix may be attributed to late adjustment of the central peak. This would occur if the rocks of the central uplift initially rose above the original plane and then subsided to their final position along secondary faults.

Structural Changes That Are a Function of Size

It is well known that a number of characteristic features of craters are size-dependent (Dence 2002). Some, such as morphology and depth-diameter ratio, change relatively abruptly at diameters that seem to be mainly a function of target material strength and gravity (Melosh 1989). Terrestrial craters in crystalline rocks change from simple to complex structure at a diameter of about 4 km and at a smaller size in weaker target materials (Dence et al. 1977). At sizes up to 25–30 km across crystalline rock, craters are progressively deeper with increasing diameter, while central peaks become increasingly more prominent. In this size range, rocks of the central peaks are conspicuously fractured and retain substantial fracture porosity, so the gravity anomalies of these craters resemble those of simple craters. Craters >30 km are of ring or peak ring morphology and considerably shallower. This is most clearly demonstrated by the two craters at Clearwater Lake, where the smaller crater is substantially deeper than its neighbor (Dence 1965). The change in form of the gravity profile at the larger crater indicates a change in the distribution of fractures, with the zone of greatest fracture porosity no longer being in the center but in the region of the ring and the peripheral trough. The concentration of fracture porosity in the peripheral trough is even more pronounced at Manicouagan (Sweeney 1978).

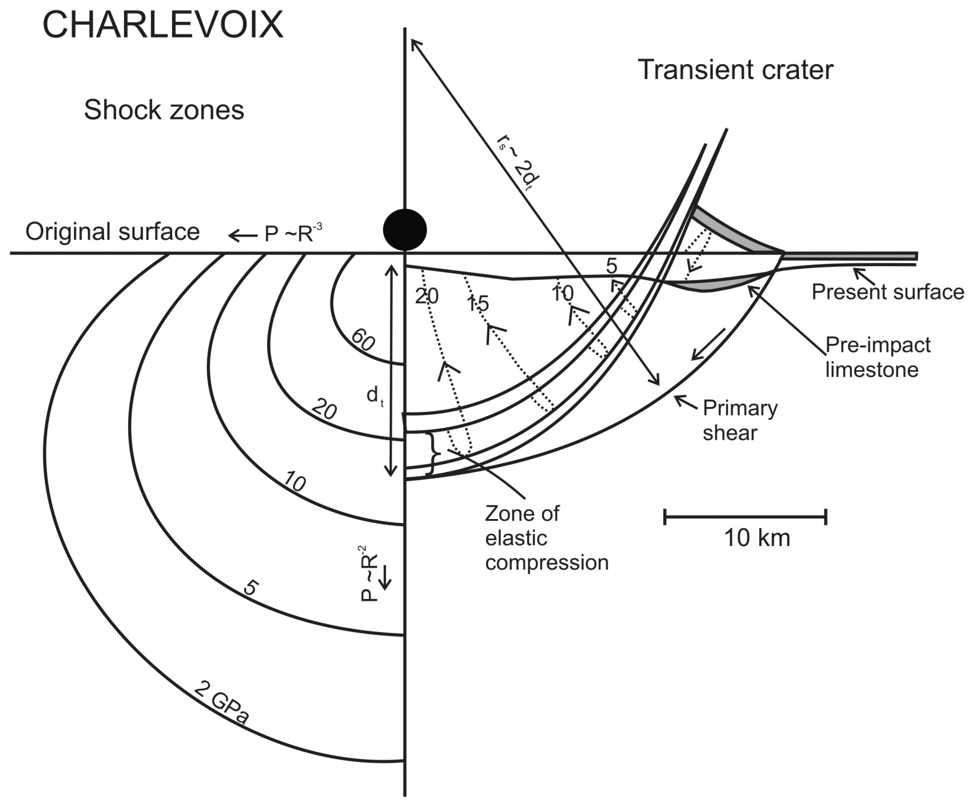

Fig. 8. Charlevoix crater cross-section. The transient crater is based on shock pressure attenuation being P ~ D^{-2} at depth down axis and P ~ D^{-3} near the surface. It is defined by the fragmentation limit, which is taken as 23–25 GPa in the center and intersecting successively lower pressure isobars at distances that give reasonable trajectories when projected to the distribution of shock metamorphism at the present surface (dotted lines). Two positions of the transient cavity wall are shown: the position defined by the procedure described above and a lower position of possible maximum depth when the compression of material below the transient crater is taken into account. It is suggested that critical stresses when the transient crater is at its maximum depth determine the position of the primary shear along which the margin collapses toward the center.

Others features seem to change smoothly with size. Of particular interest in the present context is the relationship between the fragmentation limit defining the transient crater and the imprint of shock metamorphism. While the examples of Brent and Charlevoix discussed above are the most thoroughly documented of the Canadian craters, additional information has been tabulated from other craters on the Canadian Shield (Dence 2002). The basic premise, that rocks in the central uplifts of complex craters escaped comprehensive fragmentation at the transient crater stage is clearest at the largest craters. For example, the rock exposure on the prominent topographic peaks of Mont des Éboulements at Charlevoix and Mont de Babel, Manicouagan is fair to excellent. From personal observation, it is evident that they have not been fragmented macroscopically by shock wave action, although they are shocked to pressures of about 25 GPa at Charlevoix (above) and more than 30 GPa at Manicouagan (Murtaugh 1972). This contrasts with rocks below the melt zone at Brent that have been subjected to similar pressures. There, they are strongly fragmented, allowing them to be transported across the floor of the growing transient cavity as a layer that consolidated into breccia through a combination of heat, pressure, and secondary mineralization. The rocks below the limit of fragmentation at Brent have been shocked at pressures of no more than ~7 GPa (Fig. 2). The evidence from Canadian craters that are intermediate in size between Brent and Manicouagan (Dence 2002) is that rocks from central peaks likewise exhibit intermediate shock pressures, increasing with diameter from about 10 GPa to about 25 GPa. A simple indication of change of shock metamorphic grade with size is given by the absence of maskelynite in the peaks of craters <25 km in diameter and its growing prominence in larger craters. Although the quality of these data is variable due to erosion or incomplete sampling, most pressure and diameter data are reliable within the range indicated by the limits of the symbol (Fig. 7). The firmest results come from the 9.5 km Deep Bay and 20 km Clearwater Lake East craters, where post-impact sediments have preserved the crater floor since soon after formation.

Altogether, there is a consistent trend toward higher shock pressures in the center of the parautochthone over more than 1.5 orders of magnitude in crater diameter. Using the calibration of shock metamorphism employed here, the shock pressure at the limit of fragmentation, P_L, changes with crater size as $P_L = 3.5\ D^{0.5}$, where D is the final crater diameter in km (Fig. 8). The stress field that leads to fragmentation below the zone of total shock melting requires further analysis. In Dence (2002), the fragmentation mechanism was taken to be Grady-Kipp fracturing, and the down axis limit of fragmentation was called the Grady-Kipp Limit (GPL), but here it is accepted that this terminology is inappropriate except in the near-surface region. Likewise, the reason that direct fragmentation by shock in the transient crater phase attenuates at roughly twice the rate expressed by shock metamorphism as crater size and impact energy increases needs elucidation. Numerical results, such as those of Mitani (2003), may not apply to large-scale natural impacts. It seems clear that the stresses that result in fragmentation are not directly related to those that control the formation of shatter cones that, as indicated earlier, conform to a specific range of shock pressure.

As the examples of Brent and Charlevoix illustrate (Figs. 5 and 8), this result indicates that, with increasing size, transient craters are smaller relative to the volume imprinted by the shock wave. Thus the proportion of melt to breccia within transient craters will tend to increase with size and contribute to the overall trend toward proportionally more melt being retained with increasing size (Grieve and Cintala 1992). However, the overall parabolic shape and depth-to-diameter ratio of transient craters does not seem to change substantially with size.

SYNTHESIS

The model for Brent outlined here elaborates on previous analyses (Dence 1968, 2002; Dence et al. 1977). Observation and theory have converged to give a model that demonstrates the magnitude of displacements in the early stages and the importance of slumping under gravity to the final configuration. Both are regulated by dynamic fracturing of rocks that are arguably among the strongest of natural terrestrial materials. In the excavation stage, the size of the transient crater is controlled by stresses that determine the extent of fragmentation of shock-processed target materials. In the late stage, gravitational slumping is controlled by development of the primary shear. In cross-section, the shear resembles the critical circular surface of failure along which slip develops in soils or incompetent rocks (Coates 1967), suggesting that the walls of the crater are comparably weakened by distention during uplift, allowing shear failure to take place. The center about which yielding occurs is directly over the axis of the crater, and the toe of the primary shear surface is at the bottom of the transient cavity (the mid-level of the impact melt in the case of Brent). However, it must be remembered that, while forming, the transient cavity will have a somewhat different shape, as the rim will be distended, and the rocks below the bottom of the crater will initially compress then release following transit of the shock wave.

The weight of the rim as it begins to deflate is probably the trigger that activates the primary shear and subsidiary shears. At Brent, cascading sheets slide from the crater walls into the transient crater at avalanche speeds and, in a few seconds, fill it to more than half its original depth. If the primary shear grows at the speed of sound in gneissic rocks, it would take about half a second to rupture along its length and activate the landslides. At the same time, the rocks of the parautochthone below the transient cavity, having been compressed by the shock wave in accord with their dynamic equations of state (Ahrens and Rosenberg 1968; Melosh 1989), will be expanding. The combination of elastic recovery and transformation during adiabatic release with local brecciation will result in slight expansion of the parautochthone compared with its original state. In small craters, the effect will not be large as most of the material shocked above the relevant elastic limit is fragmented and removed in the excavation process. The result depends critically on the relative rates at which these processes develop. In small craters, it seems that emplacement of the sheets cascading from the walls over the upper part of the melt zone is rapid enough to prevent any tendency for the bottom of the transient crater to rise above the level it now occupies.

Moving to the larger complex craters, at first glance there is no apparent reason that they depart from the simple crater mechanism. The gravitational collapse of the crater walls is similar, though more nearly complete than at simple craters. The apparent difference is that the primary shears converge within the parautochthone under the center rather than at the toe of the transient cavity, thereby allowing the center to rise. Why does this happen? The transient cavities, and, hence, the associated stress fields, appear to be similar. The factor that may be critical is the difference with crater size in the volume of shocked material that is fragmented and excavated (Fig. 9) and the corresponding smaller size of the transient crater relative to the energy released by impact. These results suggest a critical role for the relative rate at which events occur in the parautochthone of the transient crater.

There are several possible consequences arising from the evidence that a greater proportion of rock shocked above the Hugoniot elastic limit remains below the limit of fragmentation in large craters. In such craters, the higher level of shock pressure and the relatively greater thickness of the parautochthone below the crater floor results in elastic relaxation and transformation being proportionally more substantial. The toe of the transient cavity will be correspondingly deeper when development of the primary shear begins, assuming a similar stress field as at the smaller craters. However, the rate of formation of the primary shear will probably not scale with size, so its growth and activation will take longer. If expansion of the center occurs more rapidly than the activation of the primary shear, the center will rise before rupture occurs at the toe. Under these circumstances, slumping under gravity from the margins will drive the center

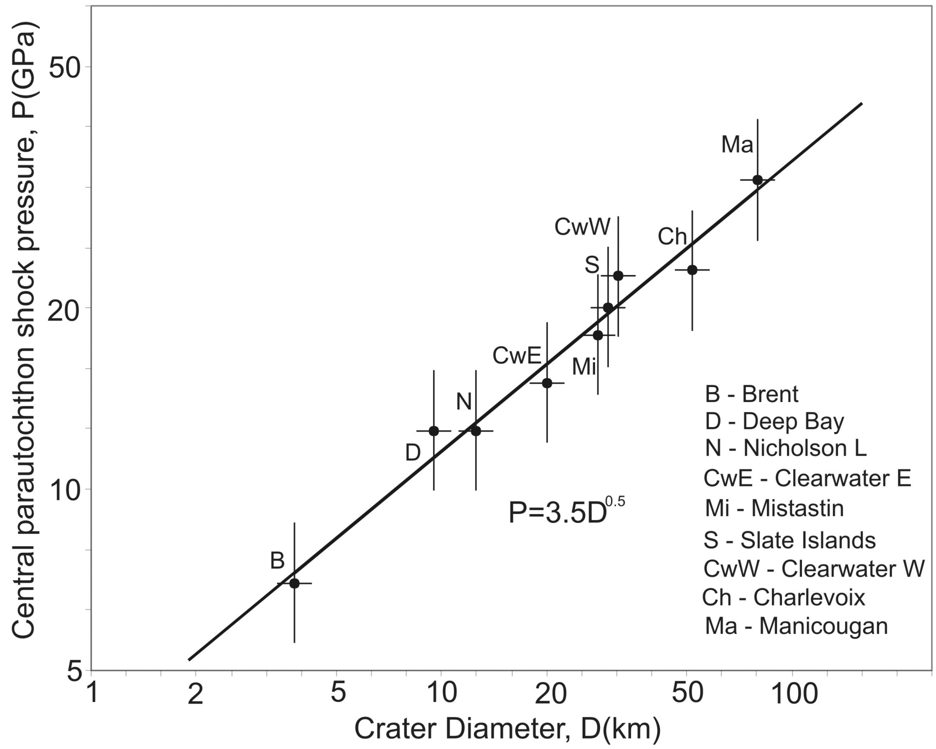

Fig. 9. Log-log plot of the relationship between the down axis limit of fragmentation and crater size, expressed as average shock pressure at the fragmentation limit (i.e., at the top of the central uplift in complex craters) versus crater diameter. P (GPa) increases with D (km) as $P = 3.5\ D^{0.5}$ (Dence 2002).

upward rather than smother the motion, as happens in simple craters. Thus, the rate at which the center rises versus the rate of rupture along the primary shear may be the determining factor in whether a central peak forms or is suppressed.

In the example of Charlevoix (Fig. 10), excavation by fragmentation reached the 25 GPa isobar at an estimated depth of 11 km. The momentary compression of the subfloor may have driven the rocks to a full depth of 13–14 km, assuming shock compression has a similar Poisson's ratio to that of elastic waves. If the transient crater reached this depth and was otherwise similar in geometry to that of Brent, the resulting stress field will favor formation of a primary shear of 26–28 km radius. If the rocks of the rim, weakened by dilation in the manner suggested for simple craters, collapse under gravity at this stage, the resulting perturbation of the stress field could limit breccia formation by fragmentation, thereby producing the observed progressive diminution of transient crater size with increasing energy. Expansion of the parautochthone following passage of the shock wave, already in progress, would allow the center to rise by a kilometer or more, depending on the rate of relaxation. The primary shear surfaces would meet well below the crater floor, driving further growth of the central uplift. This scenario has some similarity to the situation modeled by (O'Keefe and Ahrens 1993). How far uplift proceeds will depend in part on lubrication along the primary shear surfaces. Generation of friction melt will facilitate the process and is clearly of great importance in craters >30 km across, where the central uplift probably rises several kilometers above the original surface before collapsing to the present configuration. In this respect, consideration needs to be given to the role of water in facilitating melting and lubrication in the terrestrial environment compared, for example, with dry lunar conditions.

SUMMARY AND CONCLUSION

Shock metamorphism is a useful method of structural analysis, either alone or as a supplement to other evidence. The calibration in terms of gigapascals of shock pressure requires further attention, particularly regarding the effects of variations in grain size and mineralogy. The averaging method used here is relatively conservative and indicates a spread of values within single specimens on the order of 5–10 GPa, in response to shock wave interactions that amplify or diminish pressure grain by grain or within grains.

Using observations on the apparent attenuation of shock pressure, a satisfactory, direct match can be made between observation, experiment, and calculation in the case of simple impact craters, such as the Brent crater. The best fit is when actual attenuation down axis is low in the near-field region, changing in the far-field to $P \sim R^{-2}$. The relative displacement of shocked material down axis can, thereby, be calculated, as can the nominal size of the bolide and the energy released on impact.

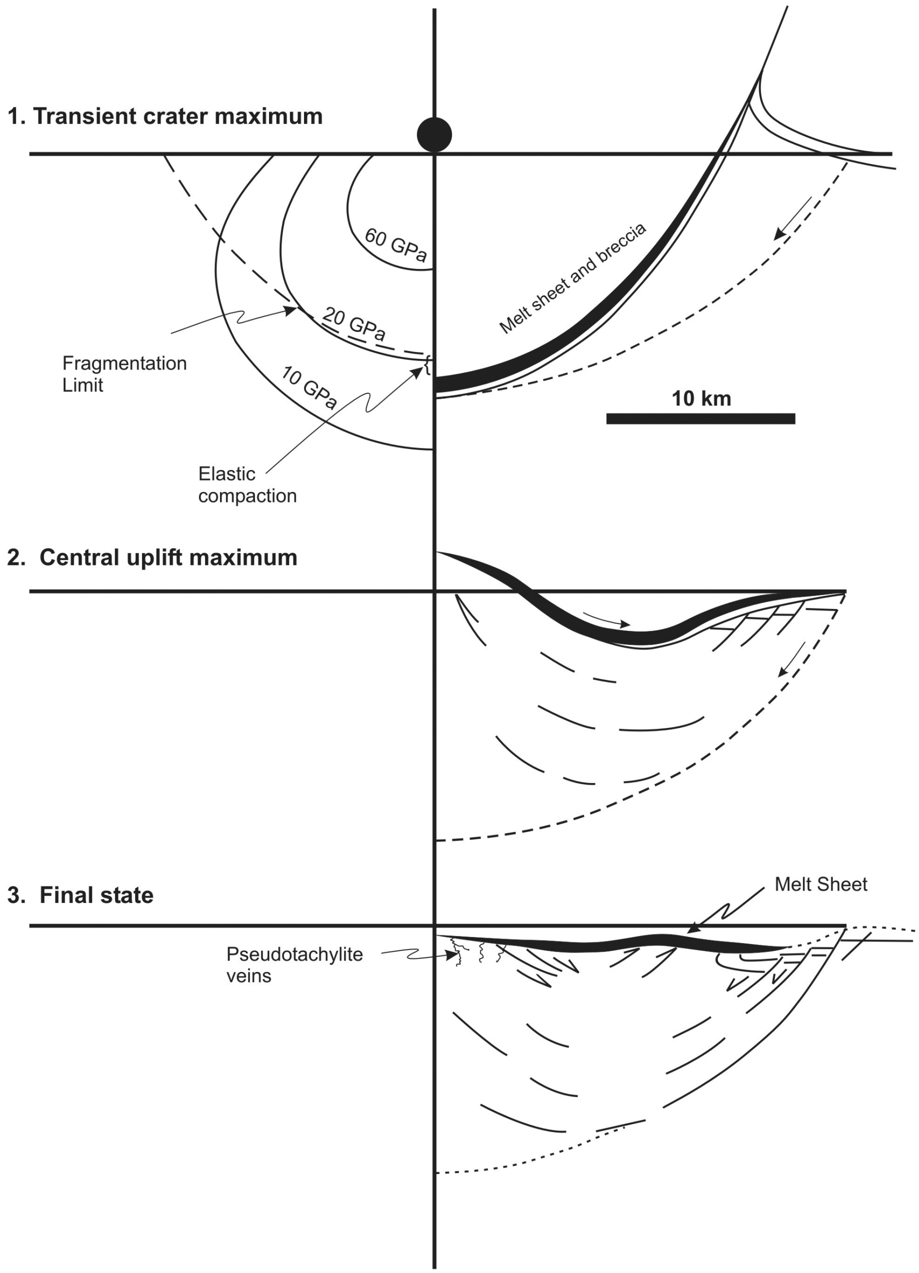

Fig. 10. Proposed Charlevoix crater model. Three stages in the development of a peak ring crater. Stage 1 repeats the transient crater stage depicted in Fig. 8. Stage 2 represents the postulated maximum development of the central uplift. Stage 3 depicts the final stage with the partial collapse of the central peak to its present state and modest uplift of the intermediate ring at the margin of the subsiding central peak. By analogy with craters where a melt sheet is preserved, a crater lining of melt and attendant breccias is shown forming in stage 1 then sliding off the central peak at stage 2 and consolidating in stage 3. Pseudotachylites formed by frictional melting and crushing along shear surfaces in stages 1 and 2 move into cracks that dilate as the central peak overshoots (stage 2) and act as a sealant as the peak subsides in stage 3. It should be noted that the central peak rocks move as large blocks, coherent over hundreds of meters, lubricated by generally thin shear zones. The total vertical motion of the center at Charlevoix is estimated to have been about 25 km.

Shear zones intersected by drilling at Brent show that, in simple craters, collapse is organized along a lowermost, primary shear surface and subsidiary overlying shears. The surface has the form of a sphere segment of radius $r_s \approx 2d_t$, where d_t is the excavated depth from the original surface to the middle of the layer of impact melt that is the floor of the transient crater. The shape of the fault is an indication that the rocks forming the walls of the transient crater have little cohesion during late stages in cavity growth and that the toe of the cavity determines the position of the zone of failure.

The primary shear, consisting of a thin layer of finely crushed and locally friction-melted rock, is interpreted as a superfault that failed rapidly. Fragmentation, additional to that due to direct shock wave action, occurred as the mass of rock sliding from the walls was emplaced above the melt zone, thereby suppressing any tendency for the floor to rise higher.

The analysis of complex craters is complementary to the simple crater situation. While little information about the near-surface region is preserved in simple craters, in complex structures, disturbance in forming the central uplift nullifies estimation of down axis shock pressure attenuation. However, the apparent rate of attenuation in rocks of the parautochthone can be observed in favorable cases like Charlevoix. If it is assumed that, as in simple craters, shock pressure attenuates down axis as $P \sim R^{-2}$, a reasonable restoration of the transient crater is achieved if the attenuation changes to approximately $P \sim R^{-3}$ in the near-surface region.

The restorations indicate that the shape of the transient crater is similar in simple and complex craters and is defined by the limit of fragmentation. In contrast to the hemispherical imprint of the shock wave, the fragmentation limit cuts shock isobars obliquely and is best depicted as parabolic. In addition, the shock pressure (in GPa) at the limit of fragmentation in the down axis direction, P_L, changes with crater size as $P_L = 3.5\ D^{0.5}$, where D (in km) is the final crater diameter. Thus, with increasing D, transient crater volume decreases relative to the volume shocked, while the volume of rock plastically and elastically deformed in the parautochthone increases relative to the shock imprint.

In larger craters, elastic compression in the relatively more strongly shocked parautochthone is important, and the transient crater may be significantly deepened. If so, $r_s \approx 2d_{te}$ may hold, where d_{te} is the effective depth of the transient crater due to both excavation to the fragmentation limit and shock compression of underlying rock. Relaxation on decompression by itself is insufficient for central peak formation, but the rise of the crater floor causes the primary shear to intersect below the fragmentation limit, allowing uplift driven by gravitational collapse of the margin to continue. The rate of collapse relative to growth of the transient crater by fragmentation is critical and requires analysis as a limitation on the volume excavated. The greater importance of pseudotachylites in large craters is witness to the exponential increase in friction melting with increasing crater size.

In terms of crater mechanics and computer simulations such as those of O'Keefe and Ahrens (1993; 1999) and Melosh and Ivanov (1999), this analysis places particular emphasis on the relatively neglected role of brittle fracturing in determining transient cavity size and late-stage adjustments under gravity. Factors that need further consideration include the concentrations of stress that favor the development of controlling fractures, the relationship between fragmentation to form breccias and shock pressure as manifest by shock metamorphism, and the rate at which fractures develop relative to exponential relaxation of plastic and elastic compression. A number of assumptions made in moving from simple to complex craters need further investigation, including the appropriate energy to diameter relationship for craters of different sizes and the validity of the assumed invariance of attenuation rates with size. Above all, it is hoped that the analysis and modeling of simple craters will attempt the difficult task of simulating observed complexities and, thus, pin point changes at the simple to complex transition and the further transition to peak ring structures.

Acknowledgments–I am grateful to the organizers of the "Bridging the Gap" workshop for their happy conception and their encouragement and financial assistance. John Spray, Lucy Thompson, James Whitehead, and colleagues at the University of New Brunswick gave me valuable support, stimulating discussions, and much needed assistance with diagrams. They are not responsible for errors of commission or omission that may be found. Boris Ivanov and Gordon Osinski provided helpful and perceptive reviews.

Editorial Handling—Dr. E. Pierazzo and Dr. R. Herrick

REFERENCES

Abels A., Plado J., Pesonen L. J,. and Lehtinen M. 2002. The impact cratering record of Fennoscandia—A close look at the database. In *Meteorite impacts in Precambrian shields,* edited by Plado J. and Pesonen L. J. Berlin: Springer-Verlag. pp. 1–58.

Ahrens T. and O'Keefe J. 1977. Equations of state and impact-induced shock-wave attenuation on the moon. In *Impact and explosion cratering,* edited by Roddy D. J., Pepin R. O., and Merrill R. B. New York: Pergamon Press. pp. 639–656.

Ahrens T. J. and Rosenberg J. T. 1968. Shock metamorphism: Experiments on quartz and plagioclase. In *Shock metamorphism of natural materials,* edited by French B. M. and Short N. M. Baltimore: Mono Book Corporation. pp. 59–81.

Baldwin R. B. 1949. *The face of the moon.* Chicago: University of Chicago Press. 239 p.

Beals C. S. 1960. A probable meteorite crater of Precambrian age at Holleford, Ontario. *Publications of the Dominion Observatory* 24(6):117–142.

Beals C. S. 1965. The identification of ancient craters. *Annals of the New York Academy of Sciences* 123:904–914.

Beals C. S., Ferguson G. M., and Landau A. 1956. A search for analogies between lunar and terrestrial topography on photographs of the Canadian shield: Part I and Part II. *Journal of the Royal Astronomical Society of Canada* 50:203–211; 250–261.

Beals C. S., Innes M. J. S., and Rottenberg J. A. 1963. Fossil meteorite craters. In *The moon, meteorites, and comets,* edited by Middlehurst B. M. and Kuiper G. P. Chicago: University of Chicago Press. pp. 235–284.

Bell K. 1985. Geochronology of the Carswell area, northern Saskatchewan. In *The Carswell structure uranium deposits, Saskatchewan,* edited by Laine R., Alonso D., and Svab M. Special Paper 29. St. Johns: Geological Association of Canada. pp. 33–46.

Bjork R. J. 1961. Analysis of the formation of Meteor Crater, Arizona: A preliminary report. *Journal of Geophysical Research* 66:3379–3387.

Borg I. Y. 1972. Some shock effects in granodiorite to 270 kilobars at the Piledriver site. In *Flow and fracture of rocks,* edited by Heard H. C., Borg I. Y., Carter N. L., and Raleigh C. B. Monograph 16. Washington D.C.: American Geophysical Union. pp. 293–311.

Bostock H. H. 1969. The Clearwater complex, New Quebec. *Geological Survey of Canada Bulletin* 178. 63 p.

Chao E. C. T. 1968. Pressure and temperature histories of impact metamorphosed rocks—Based on petrographic observations. In *Shock metamorphism of natural materials,* edited by French B. M. and Short N. M. Baltimore: Mono Book Corporation pp. 135–158.

Coates D. F. 1967. *Rock mechanics principles.* Mines Branch Monograph 874. Ottawa: Department of Energy, Mines, and Resources. 363 p.

Cooper H. F. J. 1977. A summary of explosion cratering phenomena relevant to meteor impact events. In *Impact and explosion cratering,* edited by Roddy D. J., Pepin R. O., and Merrill R. B. New York: Pergamon Press. pp. 11–44.

Currie K. L. 1971. Origin of igneous rocks associated with shock metamorphism as suggested by geochemical investigations of Canadian craters. *Journal of Geophysical Research* 76:5575–5585.

Dence M. R. 1964. A comparative structural and petrographic study of probable Canadian meteorite craters. *Meteoritics* 2:249–270.

Dence M. R. 1965. The extraterrestrial origin of Canadian craters. *Annals of the New York Academy of Sciences* 123:941–969.

Dence M. R. 1968. Shock zoning at Canadian craters: Petrography and structural implications. In *Shock metamorphism of natural materials,* edited by French B. M. and Short N. M. Baltimore: Mono Book Corporation. pp. 169–184.

Dence M. R. 1971. Impact melts. *Journal of Geophysical Research* 76:5552–5565.

Dence M. R. 1972. The nature and significance of terrestrial impact structures. Proceedings, 24th International Geological Congress, section 15. pp. 77–89.

Dence M. R. 2002. Re-examining structural data from impact craters on the Canadian shield in the light of theoretical models. In *Meteorite impacts in Precambrian shields,* edited by Plado J. and Pesonen L. J. Berlin: Springer-Verlag. pp. 59–79.

Dence M. R., Grieve R. A. F., and Robertson P. B. 1977. Terrestrial impact structures: Principal characteristics and energy considerations. In *Impact and explosion cratering,* edited by Roddy D. J., Pepin R. O., and Merrill R. B. New York: Pergamon Press. pp. 247–275.

Dence M. R. and Guy-Bray J. V. 1972. Some astroblemes, craters, and cryptovolcanic structures in Ontario and Quebec. 24th International Geological Congress Guidebook A65. Montreal. 61 p.

Dence M. R., Innes M. J. S. and Beals C. S. 1965. On the probable meteorite origin of the Clearwater Lakes, Canada. *Journal of the Royal Astronomical Society of Canada* 59(1):13–22.

Dietz R. S. 1964. Sudbury structure as an astrobleme. *Journal of Geology* 72:412–434.

Dietz R. S. 1968. Shatter cones in cryptoexplosion structures. In *Shock metamorphism of natural minerals,* edited by French B. M. and Short N. M. Baltimore: Mono Book Corporation. pp. 267–285.

Floran R. J., Grieve R. A. F., Phinney W. C., Warner J. L., Simonds C. H., Blanchard D. P., and Dence M. R. 1978. Manicouagan impact melt, Quebec. Part 1: Stratigraphy, petrology and chemistry. *Journal of Geophysical Research* 83:2737–2759.

Fredriksson K., Dube A., Milton D. J., and Balasundaran M. S. 1973. Lonar Lake, India: An impact crater in basalt. *Science* 180:862–864.

French B. M. and Short N. M. 1968. *Shock metamorphism of natural materials.* Baltimore: Mono Book Corporation. 644 p.

Gault D. E., Guest J. E., Murray J. B., Dzurisin D., and Malin M. C. 1975. Some comparisons of impact craters on Mercury and the moon. *Journal of Geophysical Research* 80:2444–2460.

Gault D. E., Quaide W. L., and Oberbeck V. R. 1968. Impact cratering mechanics and structures. In *Shock metamorphism of natural materials,* edited by French B. M. and Short N. M. Baltimore: Mono Book Corporation. pp. 87–99.

Gilbert G. K. 1896. The origin of hypotheses, illustrated by the discussion of a topographic problem. *Science* 3:1–13.

Grahn Y. and Ormö J. 1995. Microfossil dating of the Brent meteorite crater, southeast Ontario, Canada. *Revue de Micropaleontologie* 38(n. 2):131–137.

Grieve R. A. F. 1978. The melt rocks at Brent crater, Ontario, Canada. Proceedings, 9th Lunar and Planetary Science Conference. pp. 2579–2608.

Grieve R. A. F. 1998. Extraterrestrial impact on Earth: The evidence and the consequences. In *Meteorites: Flux with time and impact effects,* edited by Grady M. M., Hutchinson R., McCall G. J. H., and Rothery D. A. Special Publications 140. London: Geological Society of London. pp. 105–131.

Grieve R. A. F. and Cintala M. J. 1992. An analysis of differential impact melt-crater scaling and implications for the terrestrial impact record. *Meteoritics* 27:526–538.

Grieve R. A. F., Dence M. R., and Robertson P. B. 1977. Cratering processes: As interpreted from the occurrence of impact melts. In *Impact and explosion cratering,* edited by Roddy D. J., Pepin R. O., and Merrill R. B. New York: Pergamon Press. pp. 791–814.

Grieve R. A. F. and Garvin J. B. 1984. A geometric model for excavation and modification at terrestrial simple impact craters. *Journal of Geophysical Research* 89:11561–11572.

Grieve R. A. F., Reny G., Gurov E. P., and Ryabenko V. A. 1987. The melt rocks of the Boltysh impact crater, Ukraine, USSR. *Contributions to Mineralogy and Petrology* 96:56–62.

Grieve R. A. F. and Robertson P. B. 1976. Variations in shock deformation at the Slate Islands impact structure, Lake Superior. *Contributions to Mineralogy and Petrology* 58:37.

Grieve R. A. F., Robertson P. B., and Dence M. R. 1981. Constraints on the formation of ring structures, based on terrestrial data. In *Multi-ring basins,* edited by Schultz P. H. New York: Pergamon Press. pp. 37–57.

Halliday I. and Griffin A. A. 1967. Summary of drilling at the West Hawk Lake crater. *Journal of the Royal Astronomical Society of Canada* 61:1–8.

Hartung J. B., Dence M. R., and Adams J. A. S. 1971. Potassium-argon dating of shock metamorphosed rocks from the Brent impact crater, Ontario, Canada. *Journal of Geophysical Research* 76:5437–5448.

Hörz F. 1968. Statistical measurements of deformation structures and refractive indices in experimentally shock loaded quartz. In *Shock metamorphism of natural materials,* edited by French B. M. and Short N. M. Baltimore: Mono Book Corporation. pp. 243–253.

Hoyt W. G. 1987. *Coon Mountain controversies: Meteor Crater and the development of impact theory.* Tucson: University of Arizona Press. 442 p.

Innes M. J. S. 1961. The use of gravity methods to study the underground structure and impact energy of meteorite craters. *Journal of Geophysical Research* 66:2225–2239.

Innes M. J. S. 1964. Recent advances in meteorite crater research at the Dominon Observatory, Ottawa, Canada. *Meteoritics* 2:219–242.

Innes M. J. S., Pearson W. J., and Geuer J. W. 1964. The Deep Bay crater. *Publications of the Dominion Observatory* 31:21–51.

Ivanov B. A., Kocharyan G. G., Kostuchenko V. N., Kirjakov A. F., and Pevzner L. A. 1996. Puchezh-Katunki impact crater: Preliminary data on recovered core block structure. 27th Lunar and Planetary Science Conference. pp. 589–590.

Kelley S. P. and Gurov E. P. 2002. Boltysh, another end-Cretaceous impact. *Meteoritics & Planetary Science* 37:1031–1043.

Kranck S. H. and Sinclair G. W. 1963. Clearwater Lake, New Quebec. *Geological Survey of Canada Bulletin* 100. 25 p.

Manton W. I. 1965. The orientation and origin of shatter cones in the Vredefort ring. *Annals of the New York Academy of Sciences* 123: 1017–1049.

Meen V. B. 1950. Chubb crater, Ungava, Quebec. *Journal of the Royal Astronomical Society of Canada* 44:169–180.

Meen V. B. 1957. Chubb crater—A meteor crater. *Journal of the Royal Astronomical Society of Canada* 51:137–154.

Melosh H. J. 1989. *Impact cratering: A geological process.* Oxford: Oxford University Press. 245 p.

Melosh H. J. and Ivanov B. A. 1999. Impact crater collapse. *Annual Review of Earth and Planetary Sciences* 27:385–415.

Millman P. M., Liberty B. A., Clark J. F., Willmore P. L., and Innes M. J. S. 1960. The Brent crater. *Publications of the Dominion Observatory* 24:1–43.

Milton D. J. 1977. Shatter cones: An outstanding problem in shock mechanics. In *Impact and explosion cratering,* edited by Roddy D. J., Pepin R. O., and Merrill R. B. New York: Pergamon Press. pp. 703–714.

Milton D. J., Glikson A. Y., and Brett R. 1996. Gosses Bluff, a latest Jurassic impact structure, central Australia. Part 1: Geological structure, stratigraphy, and origin. *AGSO Journal of Australian Geology & Geophysics* 16:453–486.

Mitani N. K. 2003. Numerical simulations of shock attenuation in solids and reevaluation of scaling law. *Journal of Geophysical Research* 108:1–10.

Murtaugh J. G. 1972. Shock metamorphism in the Manicouagan cryptoexplosion structure, Quebec. In *Proceedings, 24th International Geological Congress,* edited by Millman P. M. and Dence M. R. Montreal: International Palaeontological Association. pp. 133–139.

O'Keefe J. D. and Ahrens T. J. 1993. Planetary cratering mechanics. *Journal of Geophysical Research* 98:17011–17028.

O'Keefe J. D. and Ahrens T. J. 1999. Complex craters; Relationship of stratigraphy and rings to impact conditions. *Journal of Geophysical Research* 104:27091–27104.

Palme H., Grieve R. A. F., and Wolf R. 1981. Identification of the projectile at the Brent crater and further considerations of projectile types at terrestrial craters. *Geochimica et Cosmochimica Acta* 45:2417–2424.

Robertson P. B. 1968. La Malbaie structure, Quebec—A Palaeozoic meteorite impact site. *Meteoritics* 4:89–112.

Robertson P. B. 1975. Zones of shock metamorphism at the Charlevoix impact structure, Quebec. *Bulletin of the Geological Society of America* 86:1630–1638.

Robertson P. B. 1988. The Haughton impact structure, Devon Island, Canada: Setting and history of investigations. *Meteoritics* 23: 181–184.

Robertson P. B., Dence M. R., and Vos M. A. 1968. Deformation in rock-forming minerals from Canadian craters. In *Shock metamorphism of natural materials,* edited by French B. M. and Short N. M. Baltimore: Mono Book Corporation. pp. 433–452.

Robertson P. B. and Grieve R. A. F. 1977. Shock attenuation at terrestrial impact structures. In *Impact and explosion cratering,* edited by Roddy D. J., Pepin R. O., and Merrill R. B. New York: Pergamon Press. pp. 687–702.

Roddy D. J. 1977. Large-scale impact and explosion craters: Comparisons of morphological and structural analogs. In *Impact and explosion cratering: Planetary and terrestrial implications,* edited by Roddy D. J., Pepin R. O., and Merrill R. B. New York: Pergamon Press. pp. 185–246.

Roddy D. J., Pepin R. O., and Merrill R. B., editors. 1977. *Impact and explosion cratering: Planetary and terrestrial implications.* New York: Pergamon Press. 1301 p.

Rondot J. 1966. *Geology of the La Malbaie region, Charlevoix.* Quebec Preliminary Report 544. Quebec: Department of Natural Resources. 18 p.

Rondot J. 1968. Nouvel impact météoritique fossile? La structure semi-circulaire de Charlevoix. *Canadian Journal of Earth Science* 5:1305–1317.

Rondot J. 1989. Géologie de Charlevoix. Ministère de l'Énergie et des Ressources du Québec. 19 cartes + 606 p.

Shoemaker E. M. 1960. Penetration mechanics of high velocity meteorites, illustrated by Meteor crater, Arizona. In *Report of the XXIst International Geological Congress, Norden.* Copenhagen: International Geological Congress. pp. 418–434.

Shoemaker E. M. 1963. Impact mechanics at Meteor crater, Arizona. In *The moon, meteorites, and comets,* edited by Middlehurst B. M. and Kuiper G. P. Chicago: University of Chicago Press. pp. 301–336.

Short N. M. 1968. Nuclear-explosion-induced microdeformation of rocks: An aid to the recognition of meteorite impact structures. In *Shock metamorphism of natural materials,* edited by French B. M. and Short N. M. Baltimore: Mono Book Corporation. pp. 185–210.

Short N. M. 1970. The anatomy of a meteorite impact crater: The West Hawk Lake structure, Manitoba, Canada. *Bulletin of the Geological Society of America* 81:609–648.

Spray J. 1997. Superfaults. *Geology* 25:627–630.

Spray J. G. 1998. Localized shock- and friction-induced melting in response to hypervelocity impact. In *Meteorites: Flux with time and impact effects,* edited by Grady M. M., Hutchison R., McCall G. J. H., and Rothery D. A. London: Geological Society of London. pp. 195–204.

Stöffler D. 1966. Zones of impact metamorphism in the crystalline rocks of the Nördlinger Ries crater. *Contributions to Mineralogy and Petrology* 12:15–24.

Sweeney J. F. 1978. Gravity study of great impact. *Journal of Geophysical Research* 83:2809–2815.

von Engelhart W. and Stöffler D. 1968. Stages of shock metamorphism in crystalline rocks of the Ries Basin, Germany. In *Shock metamorphism of natural materials,* edited by Short N. M. Baltimore: Mono Book Corporation. 644 p.

Wanless R. K., Stevens R. D., Lachance G. R., and Edmonds C. M. 1968. *Age determinations and geological studies, K-Ar isotopic ages, report 8.* Paper 67-2, Part A. Ottawa: Geological Survey of Canada. 141 p.

Willmore P. L. 1963. The seismic investigation of the Manicouagan-Mushalagan Lake area in the province of Quebec. *Publications of the Dominion Observatory* 27:325–336.